NIH Public Access
Author Manuscript
J Immunol. Author manuscript; available in PMC 2013 October 15.

Published in final edited form as:
J Immunol. 2012 October 15; 189(8): 4165–4174. doi:10.4049/jimmunol.1201241.

B7x in the periphery abrogates pancreas specific damage mediated by self-reactive CD8 T cells

Jun Sik Lee[*,1,2], **Lisa Scandiuzzi**[*,1], **Anjana Ray**[*], **Joyce Wei**[†], **Kimberly A. Hofmeyer**[*], **Yael M. Abadi**[*], **P'ng Loke**[‡], **Juan Lin**[§], **Jianda Yuan**[†], **David V. Serreze**[¶], **James P. Allison**[†], and **Xingxing Zang**[*]

[*]Department of Microbiology and Immunology, Albert Einstein College of Medicine, Bronx, NY 10461

[§]Department of Epidemiology, Albert Einstein College of Medicine, Bronx, NY 10461

[†]Howard Hughes Medical Institute, Department of Immunology, Ludwig Center for Cancer Immunotherapy, Memorial Sloan-Kettering Cancer Center, New York, NY 10065

[‡]Department of Medical Parasitology, New York University School of Medicine, New York, NY 10010

[¶]The Jackson Laboratory, Bar Harbor, ME 04609

Abstract

B7x (B7-H4 or B7S1) is the seventh member of the B7 family and the *in vivo* function remains largely unknown. Despite new genetic data linking the *B7x* gene with autoimmune diseases, how exactly it contributes to peripheral tolerance and autoimmunity is unclear. Here we showed that B7x protein was not detected on antigen-presenting cells or T cells in both human and mice, which is unique in the B7 family. As B7x protein is expressed in some peripheral cells such as pancreatic β cells, we utilized a CD8 T cell-mediated diabetes model (AI4αβ) in which CD8 T cells recognize an endogenous self-antigen, and found that mice lacking B7x developed more severe diabetes than control AI4αβ mice. Conversely, mice overexpressing B7x in the β cells (Rip-B7xAI4αβ) were diabetes free. Furthermore, adoptive transfer of effector AI4αβ CD8 T cells induced diabetes in control mice, but not in Rip-B7xAI4αβ mice. Mechanistic studies revealed that pathogenic effector CD8 T cells were capable of migrating to the pancreas but failed to robustly destroy tissue when encountering local B7x in Rip-B7xAI4αβ mice. Although AI4αβ CD8 T cells in Rip-B7xAI4αβ mice and AI4αβ mice showed similar cytotoxic function, cell death, and global gene expression profiles, these cells had greater proliferation in AI4αβ mice than in RIP-B7xAI4αβ mice. These results suggest that B7x in nonlymphoid organs prevents peripheral autoimmunity partially through inhibiting proliferation of tissue-specific CD8 T cells and that local overexpression of B7x on pancreatic β cells is sufficient to abolish CD8 T cell-induced diabetes.

Introduction

The interaction between the B7 family and their receptor CD28 family generates positive costimulation and negative coinhibition which are necessary for the regulation of peripheral T cell activation and tolerance. B7x (B7-H4 or B7S1) is the seventh member of the B7

Address correspondence and reprint requests to Dr. Xingxing Zang, Department of Microbiology and Immunology, Albert Einstein College of Medicine, 1300 Morris Park, Avenue, Forchheimer Building 405, Bronx, NY 10461. xingxing.zang@einstein.yu.edu.
[1]J.S.L., and L.S. contributed equally to this work
[2]Present address: Department of Biology, College of Natural Science, Chosun University, Gwangju 501-759, South Korea.

NIH-PA Author Manuscript
NIH-PA Author Manuscript
NIH-PA Author Manuscript

NIH-PA Author Manuscript

NIH-PA Author Manuscript

NIH-PA Author Manuscript

family and is able to inhibit *in vitro* T cell proliferation and cytokine production in the presence of TCR signaling (1–3). In contrast to classical B7-1 and B7-2 whose expression is generally limited to professional antigen-presenting cells (APCs) in lymphoid organs, B7x mRNA is detected more highly in nonlymphoid organs than lymphoid organs (1, 4). The combination of the *in vivo* mRNA expression pattern and the *in vitro* T cell coinhibitory capability of B7x suggests that the B7x pathway may be important in regulating tolerance and autoimmunity in nonlymphoid organs.

Most autoimmune diseases are genetically complex, and variation at a large number of genes influences disease susceptibility and progression (5, 6). Type 1 diabetes (T1D), an autoimmune disease, is characterized by self-reactive T cells that recognize and destroy the insulin-producing β cells of the pancreas, resulting in a breakdown of glucose homeostasis. Genetic mapping and gene-phenotype studies in mice and humans have revealed that, in addition to the MHC locus, more than 20 insulin-dependent diabetes (Idd) loci contribute to T1D development (7). One of these loci, the Idd10 locus on mouse chromosome three, contains the *B7x* gene (8), suggesting a potential role of B7x in T1D. Murine studies support this notion as B7x suppresses CD4 T cell-mediated T1D (4). Juvenile idiopathic arthritis, another autoimmune disease, is the most common chronic rheumatic disease of childhood, and the majority of genetic risk factors remain to be elucidated. Recently a genome-wide association analysis identifies 10 single-nucleotide polymorphisms (SNPs) in non-coding regions of the *B7x* gene that are strongly associated with juvenile idiopathic arthritis (9). In addition, two SNPs in the *B7x* gene are significantly associated with increased serum IgE in children (10). Despite these recently discovered genetic data linking the *B7x* gene to different autoimmune diseases, it is unclear how B7x contributes to peripheral tolerance and autoimmunity.

In this study, we found that endogenous B7x protein was not detected on APCs and T cells of either human or mouse. As B7x protein is expressed on pancreatic β cells (4), we crossed B7x deficient mice (B7x−/−) or transgenic mice over-expressing B7x in pancreatic β cells (Rip-B7x) (4) with CD8 TCR transgenic mice (AI4αβ) specific for an antigen expressed by pancreatic β cells (11, 12) to study the role of tissue-expressed B7x in CD8 T cell-mediated organ-specific autoimmune destruction. B7x−/− mice developed exacerbated diabetes induced by β cell antigen-specific AI4αβ CD8 T cells, whereas over-expression of B7x on pancreatic β cells was sufficient to completely abrogate diabetes induced by the same antigen-specific CD8 T cells. In addition, Rip-B7x transgenic mice were resistant to diabetes induced by adoptive transfer of effector AI4αβ CD8 T cells. The absence of diabetes in Rip-B7x transgenic mice was not due to a primary defect in cytotoxic function of pathogenic CD8 T cells, but rather, was most likely due to the inhibitory effect of tissue-expressed B7x on proliferation of pathogenic CD8 T cells.

Material and Methods

Mice

B7x−/−, Rip-B7x, AI4α/B6.H2$^{g7/g7}$, and AI4β/B6.H2$^{g7/g7}$ mice were previously described (4, 13). B7x−/− mice were crossed to C57BL/6.H2$^{g7/g7}$ background, and then crossed to AI4α/B6.H2$^{g7/g7}$ or AI4β/B6.H2$^{g7/g7}$ to get B7x−/−AI4α/B6.H2$^{g7/g7}$ or B7x−/−AI4β/B6.H2$^{g7/g7}$ which were further intercrossed to generate B7x−/−AI4αβ/B6.H2$^{g7/g7}$. Rip-B7x mice were crossed to C57BL/6.H2$^{g7/g7}$ background, and then crossed to AI4α/B6.H2$^{g7/g7}$ or AI4β/B6.H2$^{g7/g7}$ to get Rip-B7xAI4α/B6.H2$^{g7/g7}$ or Rip-B7xAI4β/B6.H2$^{g7/g7}$ which were further intercrossed to generate Rip-B7xAI4αβ/B6.H2$^{g7/g7}$. All mice were maintained under specific pathogen-free conditions at the Albert Einstein College of Medicine following protocols approved by the Institutional Animal Care and Use Committee.

NIH-PA Author Manuscript

NIH-PA Author Manuscript

NIH-PA Author Manuscript

Antibodies and tetramer for flow cytometry

Cells were preincubated with anti-CD16/CD32 and then stained with antibodies against B7x [clones 9 and H74, eBioscience; BAF2154, RD System; our own clone 19D6, 15D12, 12D11, and 1H3 (4)] or other markers (eBioscience, BD Pharmingen, AbD Serotec). For intracellular staining, cells were fixed, permeabilized, and then stained. Alexa647-conjugated MimA2 (YAIENYLEL)/H-2D^b tetramer was made by the NIH Tetramer Core Facility. Alive and dead cells were detected using LIVE/DEAD marker (Invitrogen). Samples were examined using a FACSCalibur or LSRII (BD Biosciences) with subsequent analysis of data in FlowJo (Treestar).

Stimulation of immune cells

Human peripheral blood mononuclear cells (PBMC) were isolated by Ficoll-Hypaque gradient centrifugation and T cells were stimulated with PHA (5 μg/ml) for 72h or PMA (50 ng/ml) and ionomycin (1 μg/ml) for 48h. B cells were purified from PBMC with CD19 MicroBeads (Miltenyi Biotec) and activated with LPS (60 μg/ml) for 72h or PMA/ionomycin for 36h. Monocytes were purified from PBMC with CD14 MicroBeads and activated with LPS (100 ng/ml) and IFN-γ (100 ng/ml) for 36h. Monocyte-derived Dendritic cells (DCs) and CD34-derived Langerhans cells (LCs) were generated and activated with CD40L (soluble rhuCD40-L trimer, 0.5 μg/ml; Immunex), LPS (60 μg/ml), PMA (50ng/ml)/ionomycin (1 μg/ml), or cytokine cocktail (2 ng/ml IL-1β, 1000 IU/ml IL-6, 10 ng/ml TNF-α and 5 mM/ml PGE_2) as described (14). Mouse T cells were stimulated with ConA (0.02–20 μg/ml) or plate-coated anti-CD3/CD28 (0.1–40 μg/ml) for 72h, or PMA/ionomycin for 48h. Th1 and Th2 cell lines were generated from OT-II mice as described (15). B cells were activated with LPS (2.5–80 μg/ml) or anti-IgM $F(ab')_2$ fragment (2.5–80 μg/ml) for 72h, or PMA/ionomycin for 48h. Nematode *Brugia malayi* infection-induced alternatively activated macrophages and DCs were obtained as described (16). Infiltrating immune cells in the lung from 4T1-induced lung metastasis or *Streptococcus pneumoniae*-induced lung (17) infection were also used.

Assessment of diabetes development

Diastix (Bayer) testing strips were used to determine urine glucose levels in mice. Mice were considered diabetic after two consecutive measurements exceeding 250 mg/dl.

Histology and immunohistochemistry

Mouse organs were fixed with 4% paraformaldehyde and embedded in paraffin. Sections were stained with hematoxylin and eosin (HE) or Gomeri aldehyde-fuchsin (GAF) staining for pancreatic β cells by the Histotechnology and Comparative Pathology Core Facility. For immunohistochemical staining, tissues were collected from mice and fixed in 10% neutral buffered formalin (NBF) (Fisher) prior to paraffin embedding. Following clearing in xylene washes and rehydration, antigen retrieval was performed in a vegetable steamer in Tris/EDTA antigen retrieval solution. Sections were biotin blocked using the ScyTek Biotin Blocking kit and then normal blocking was done using horse serum (Vector Labs). Sections were incubated with a biotinylated anti-B7-H4 Ab or isotype IgG control (R&D Systems) overnight at 4°C and then blocked for endogenous peroxidase for 10 min in 1% H_2O_2. Sections were incubated in ABC reagent (Vector Labs) for 20 min, then the tyramide amplification kit (Invitrogen) was used, followed again with the ABC reagent for 20 min. Sections were developed with the DAB kit (Vector Labs), counterstained with hematoxylin, dehydrated, cleared in xylene and mounted.

NIH-PA Author Manuscript

NIH-PA Author Manuscript

NIH-PA Author Manuscript

Adoptive transfer of AI4αβ CD8 T cells

2×10^7 splenocytes from AI4αβ/B6$^{g7/g7}$ mice were injected intravenously into sublethally irradiated mice (750 rads) as described (18), and recipients were monitored for diabetes. Alternatively, splenocytes from AI4αβ/B6$^{g7/g7}$ mice were stimulated with MimA2 peptide (3.5 μg/ml), irradiated C57BL/6.H2$^{g7/g7}$ splenocytes (2000 rads), LPS (0.18 μg/ml) and IL-2 (10 U/ml) for 5 days. The activated AI4αβ CD8 T cells were then transferred intravenously into mice at 5×10^6 per mouse, and recipients were monitored for diabetes.

Cell-mediated cytotoxicity assay

CD8 T cells (>95% AI4αβ cells) from AI4αβ and Rip-B7xAI4αβ mice were purified with Miltenyi beads, and then incubated with MimA2 peptide-pulsed and PKH-26/CFSE-labeled C57BL/6.H2$^{g7/g7}$ splenocytes for 4 h. The percent-specific cytotoxicity was determined as described (19).

Microarray analysis

Pancreata from mice were chopped in RPMI with 5% FCS and proteinase inhibitors and then incubated at 37°C in digestion buffer (50 mL RPMI, 5% FCS, 1 mL collagenase IV, 2 U/mL DNAse I, and 100μL heparin) for 10 min. After filtering through 40 μm strainers, single-cell suspensions were pooled and AI4αβ CD8 T cells were isolated by FACS sorting using anti-CD8 Ab and MimA2/H-2D^b tetramer (99% purity of sorted AI4αβ cells) and then immediately placed in RNAlater (Qiagen). Samples were assessed with Affymetrix Mouse Gene 1.0 ST array chips by Genomics Core Facility. Microarray data were deposited in the Gene Expression Omnibus (http://www.ncbi.nlm.nih.gov/geo/) under accession number GSE40225. The array data were imported into Expression Console v1.1 (Affymetrix), normalized after quality control, and ranked using LIMMA (R package) analysis for comparison of different groups. Three technical replicates for each group were averaged for fold-change and statistical significance was set to $p<0.05$ by applying *t*-test analysis adjusted for multiple comparisons.

Statistical analyses

Statistical significance was calculated with the unpaired *t*-test using Prism software version (GraphPad). A p value of < 0.05 was considered statistically significant.

Results

B7x protein is not expressed on antigen-presenting cells or T cells in both human and mice

As all other B7 family members are mainly expressed on APCs, we wanted to determine whether B7x protein was detected on human APCs and T cells. Using a panel of monoclonal antibodies (Abs) and a polyclonal Ab, we failed to detect B7x protein with flow cytometry on B cells, monocytes, and T cells from PBMC before or after stimulation: monocytes with LPS/IFN-γ, B cells with LPS or PMA/ionomycin, and T cells with PHA or PMA/ionomycin (Table I). These stimuli were able to up-regulate the expression of B7-H1 (PD-L1) or B7-2 (Supplementary Fig. 1A–C), but not B7x (Table I). Similarly, no B7x protein was detected on human immature DCs, immature LCs, as well as mature DCs or mature LCs stimulated with cytokine cocktail, CD40L, LPS or PMA/ionomycin (Table I). In contrast, B7-2 was significantly up-regulated on mature DCs and LCs as the results of activation and maturation (Supplementary Fig. 1D, E). As positive controls, anti-B7x Abs stained a human B7x-transfected 293 cell line (Supplementary Fig. 1F). We recently reported that among 103 ovarian borderline tumors and carcinomas tested, all expressed B7x (20). The tumor-

NIH-PA Author Manuscript

NIH-PA Author Manuscript

NIH-PA Author Manuscript

infiltrating lymphocytes we observed in some of these samples, however, were B7x negative.

We recently show that murine DCs or macrophages do not express B7x protein *in vitro* even after culturing in various stimulating, suppressive, and maturation conditions (4). We further isolated B and T cells and incubated them with various stimuli: B cells with LPS, anti-IgM F(ab')2, PMA/ionomycin; T cells with ConA, plate-bound anti-CD3/CD28, PMA/ ionomycin as well as T cell subpopulations of Th1, Th2 and Treg. We did not detect B7x protein expression on these stimulated cells (Table I). In contrast, PD-1 was induced on activated T and B cells (Supplementary Fig. 2A,B). In addition, we were unable to detect B7x protein in DCs and alternatively activated macrophages from chronic *Brugia malayi* infection (16) or immune cells from *Streptococcus pneumoniae*-induced lung infection (17). Leukocytic infiltrates in 4T1-induced lung metastatic cancer were also B7x negative (Table I). In contrast, DCs and alternatively activated macrophages from chronic *Brugia malayi* infection expressed high levels of PD-L2 (Supplementary Fig. 2C). As a positive control, a BWZ cell line overexpressing mouse B7x stained well with anti-B7x in flow cytometry (Supplementary Fig. 2D). Collectively, these results demonstrate that, unlike any other B7 molecules, endogenous B7x protein is not expressed in the immune cells of either human or mouse.

More aggressive CD8 T cell-mediated tissue destruction in B7x-deficient mice

B7x protein is expressed in mouse pancreatic β cells (4) and human pancreas (21). To dissect the *in vivo* function of B7x, we generated B7x−/− mice which were born at the expected Mendelian frequency, and were of normal size, maturation and fertility. We found that B7x−/− mice developed more severe diabetes than wild-type control mice after the injection of activated diabetogenic BDC2.5 CD4 T cells (4). It is unknown, however, whether tissue-expressed B7x is able to regulate CD8 T cell function *in vivo*. Therefore, we investigated the function of endogenous B7x in CD8 T cell-mediated tissue destruction. To address this, we took advantage of AI4αβ transgenic mice that carry the rearranged TCR α and β chain genes (Vα8Vβ2) from a NOD-derived MHC class I-restricted CD8 T cell clone (11). AI4αβ CD8 T cells recognize an epitope from dystrophia myotonica kinase expressed by pancreatic β cells (12) and are capable of killing β cells and mediating overt diabetes on the C57BL/6.H2$^{g7/g7}$ background in the complete absence of CD4 T cell help (22). We crossed B7x−/− mice to the C57BL/6.H2$^{g7/g7}$ background, then crossed to AI4αβ mice (Fig. 1A) and monitored diabetes development in B7x−/−AI4αβ and AI4αβ mice (Fig. 1B–D). We observed that the disease onset (the first day when glucose level exceeded 250 mg/dl) and the point at which 100% of mice had developed diabetes came approximately 2–4 days earlier in B7x−/−AI4αβ mice than AI4αβ controls (Fig. 1B). This trend resulted in higher average glucose levels in B7x−/−AI4αβ mice (Fig. 1C). Furthermore, more aggressive disease progression in B7x−/−AI4αβ mice resulted in earlier mortality; these mice started to die roughly 16 days earlier than controls (Fig. 1D). Considering that naïve B7x−/− mice were healthy and that B7x deficiency in AI4αβ mice resulted in more aggressive disease, these results suggest that the role of B7x in T cell regulation mainly lies in disease progression but not in the naïve steady state.

Local expression of B7x completely abrogates CD8 T cell-mediated diabetes

In AI4αβ mice, CD8 T cells are able to destroy pancreatic β cells and induce an aggressive onset of diabetes with 100% of mice exhibiting disease, and all mice ultimately die within two months. B7x−/−AI4αβ mice developed T1D earlier even than AI4αβ control mice. Moreover, nearly half of B7x−/−AI4αβ mice died by day 12 (Fig. 1D), which made it extremely difficult to obtain enough AI4αβ CD8 T cells from these mice for further functional assays. Therefore, we next examined whether B7x overexpressed in pancreatic β

NIH-PA Author Manuscript

NIH-PA Author Manuscript

NIH-PA Author Manuscript

cells could regulate CD8 T cell-mediated tissue destruction and disease development *in vivo*. Rip-B7x transgenic mice overexpress B7x in pancreatic β cells under the rat insulin II promoter (4). We crossed Rip-B7x mice to the C57BL/6.H2$^{g7/g7}$ background, then crossed to AI4αβ mice (Fig. 1A) and monitored diabetes in Rip-B7xAI4αβ and AI4αβ mice (Fig. 1B–D). We found that while Rip-B7xAI4αβ mice did not succumb to diabetes and remained healthy indefinitely, all AI4αβ mice developed diabetes and died within 50 days. Compared to diabetes-free Rip-B7xAI4αβ mice, AI4αβ mice had lower body weight and smaller pancreas, pancreatic lymph nodes, and spleen. These findings clearly demonstrate that local overexpression of B7x is sufficient to completely abolish tissue destruction induced by autoimmune CD8 T cells *in vivo*.

Pathogenic CD8 T cells infiltrate to the pancreas in B7x-transgenic mice

During the pathogenesis of diabetes, islet antigen-specific T cells are activated in pancreatic lymph nodes by APCs (23–25). Subsequently, T cells infiltrate into pancreatic islets (insulitis) and eventually cause overt diabetes. One interpretation for the absence of diabetes in Rip-B7xAI4αβ mice is that pathogenic CD8 T cells are unable to migrate from lymphoid tissues into the pancreas in B7x-transgenic mice. To assess this possibility, we first examined the development of insulitis in Rip-B7xAI4αβ and AI4αβ mice. HE stained pancreatic sections from around 30-day-old mice showed that Rip-B7xAI4αβ mice, like naïve C57BL/6.H2$^{g7/g7}$ mice, maintained normal islet architecture, whereas AI4αβ mice lost almost all islets (Fig. 2A, upper panel). However, about 23% of islets in transgenic Rip-B7xAI4αβ mice had leukocytic infiltrates. We further used GAF staining to visualize β cells and found that the majority of islets in Rip-B7xAI4αβ mice were intact and completely GAF-staining positive (Fig. 2A, middle panel), however, some islets had only partial GAF-positive staining (Fig. 2A, lower panel). Pancreas of AI4αβ mice barely contained intact islets and therefore no GAF-positive staining was detected (Fig. 2A). Unlike the pancreas, no notable leukocyte infiltration was observed in other nonlymphoid organs such as the brain, kidney, liver, and lung in both Rip-B7xAI4αβ and AI4αβ mice (Fig. 2B). These observations indicate that leukocytes are able to specifically infiltrate the pancreas of Rip-B7xAI4αβ mice.

To obtain a more complete picture, we analyzed the leukocytic infiltrates from the pancreas. Single-cell suspensions prepared from the pancreas, pancreatic lymph node, and spleen were stained with MimA2/H2-D^{b} tetramer and anti-CD8 Ab to detect AI4αβ cells (18) and with lineage-specific antibodies to examine other immune cells. More than 95% of CD8 T cells were tetramer positive in AI4αβ and Rip-B7xAI4αβ mice. Flow cytometry analysis showed that there were fewer AI4αβ cells in the pancreas and pancreatic lymph node of Rip-B7xAI4αβ mice than AI4αβ mice (Fig. 3A), although the difference did not reach statistical significance. In addition, there was no significant difference in the number of other immune cells, including CD4 T cells, B cells, NK cells, DCs, macrophages, and neutrophils in the pancreas, pancreatic lymph node (PLN) and spleen between Rip-B7xAI4αβ mice and AI4αβ mice. These data suggest that the infiltration of other immune cells in the pancreas do not significantly contribute to the phenotypic difference between Rip-B7xAI4αβ and AI4αβ mice.

As about 23% of islets in transgenic Rip-B7xAI4αβ mice had leukocytic infiltrates, we asked whether the infiltrate could affect the B7x expression in islets of these mice. Immunohistochemistry analysis revealed that most islets had strong expression of B7x protein throughout (Fig. 3B, upper panel); however, in islets with leukocytic infiltrates B7x-positive cells were confined to areas devoid of infiltrates (Fig. 3B, upper panel), indicating a reverse correlation between B7x expression and leukocytic infiltration. As expected, pancreatic islets in AI4αβ mice were barely detectable with no obvious staining for B7x (Fig. 3B, lower panel).

NIH-PA Author Manuscript

NIH-PA Author Manuscript

NIH-PA Author Manuscript

Taken together, these results suggest that AI4αβ T cells in the pancreas and pancreatic lymph node, but not other immune cells, were associated with the disease. These observations also rule out the possibility that the absence of diabetes in B7x-transgenic mice was due to a primary defect in the ability of pathogenic CD8 T cells to infiltrate the pancreas.

B7x inhibits effector CD8 T cell-induced diabetes

In order to examine whether local overexpression of B7x is able to inhibit effector CD8 T cell-induced autoimmune damage, we utilized an adoptive transfer model of diabetes in which splenocytes from AI4αβ mice induced the disease in irradiated recipients (18). Splenocytes were isolated from 25–30 day old AI4αβ mice and transferred to sublethally irradiated mice at 2×10^7 cells per mouse (Fig. 4A). C57BL/6.H2$^{g7/g7}$ recipients started to develop diabetes around day 10 and all progressed to the disease around day 20 (Fig. 4B–C). In contrast, no RIP-B7x recipients on C57BL/6.H2$^{g7/g7}$ background succumbed to the disease (Fig. 4B–C). HE stained pancreatic sections from around 30 days after splenocyte transfer revealed that Rip-B7x mice had fewer leukocytic infiltrates and more normal islet architecture than C57BL/6.H2$^{g7/g7}$ mice (Fig. 4D). Similarly, Rip-B7x recipients exhibited more GAF-positive staining than C57BL/6.H2$^{g7/g7}$ recipients (Fig. 4D).

Irradiation of mice usually induces profound changes including cell death and inflammation, which could complicate behavior and function of adoptively transferred T cells *in vivo*. Therefore, we developed a new “clean” system in which adoptively transferred CD8 T cells were capable of yielding 100% diabetes in naïve, non-irradiated recipients. Splenocytes isolated from AI4αβ mice were activated with MimA2 peptide and APCs in the presence of IL-2 and LPS for five days, which led to the expansion of effector AI4αβ cells with low CD62L expression (data not shown). Adoptive transfer of 5×10^6 effector AI4αβ cells per mouse (Fig. 5A) rapidly induced diabetes in all C57BL/6.H2$^{g7/g7}$ recipients within one week (Fig. 5B–C). Again, none of the RIP-B7x recipients on C57BL/6.H2$^{g7/g7}$ background succumbed to the disease (Fig. 5B–C). 30 days after adoptive transfer of effector AI4αβ cells, we further prepared single-cell suspensions from pancreas, pancreatic lymph node, and spleen to identify AI4αβ cells using MimA2/H2-D^b tetramer and an anti-CD8 Ab. Compared to control C57BL/6.H2$^{g7/g7}$ mice, Rip-B7x mice had significantly lower numbers of AI4αβ cells in the pancreas (Fig. 5D).

Taken together, the results from these two adoptive transfer models of diabetes demonstrate that B7x overexpressed in pancreatic β cells abrogates diabetes by halting effector CD8 T cell-mediated tissue destruction.

Global gene expression and functional molecules in pancreatic CD8 T cells

To further understand the molecular mechanisms by which local expression of B7x abrogates effector CD8 T cell-mediated tissue destruction, we undertook a microarray analysis of AI4αβ cells from the pancreas. Single-cell suspensions prepared from pancreas from ten 25–30-day old AI4αβ or Rip-B7xAI4αβ mice were pooled and AI4 CD8 T cells were isolated by FACS-sorting using MimA2/H2-Db tetramer and an anti-CD8 Ab. Triplicate samples from a total of 20–30 AI4αβ or Rip-B7xAI4αβ mice were analyzed with microarrays containing more than 35,000 mouse transcripts. By using high-stringency criteria for evaluation ($p < 0.05$, and changes of two-fold or greater as cutoffs), we found, unexpectedly, that only one gene transcript, *Ccl3* (MIP-1α), was differentially regulated in pancreatic AI4αβ CD8 T cells in Rip-B7xAI4αβ mice versus control AI4αβ mice (Fig. 6A–B). Consistent with the microarray results, RT-PCR detected a significant amount of *Ccl3* mRNA in pancreatic AI4αβ CD8 T cells from Rip-B7xAI4αβ mice but not from AI4αβ mice (Fig. 6B). These data show that pancreatic effector CD8 T cells in Rip-B7xAI4αβ and

NIH-PA Author Manuscript

NIH-PA Author Manuscript

NIH-PA Author Manuscript

AI4αβ mice have a similar pattern of global gene expression and that genetic signatures of these T cells are nearly indistinguishable.

We next analyzed some key functional molecules in AI4αβ T cell at the protein level. Single-cell suspensions prepared from the pancreas, pancreatic lymph node, and spleen were stained with MimA2/H2-D^b tetramer for AI4αβ cells and with Abs against functional molecules. Granzyme B (GzmB) is the most abundant component of the cytolytic granule and is a major part of the cytolytic mechanisms enabled by perforin (26). IFN-γ up-regulates MHC class I expression on the β cells (27, 28), and together with IL-1β or TNF-α, induces β cell apoptosis (29). IFN-γ is considered traditionally as a proinflammatory factor. However, studies also reveal IFN-γ's anti-inflammatory effects in some autoimmune diseases (30, 31). We examined these two cytotoxic effector molecules in AI4αβ cells by intracellular staining. In spleen and pancreatic lymph node, the expression levels of GzmB and IFN-γ in AI4αβ cells from Rip-B7xAI4αβ mice were comparable with those from AI4αβ mice (Fig. 6C). In the pancreas, GzmB levels were similar while IFN-γ was higher in Rip-B7xAI4αβ mice than AI4αβ mice but did not reach significant difference (Fig. 6C). As both groups of mice had low percentages of pancreatic IFN-γ-producing AI4αβ cells (Fig. 6C), it was unlikely that such a low amount of IFN-γ without significant difference would markedly contribute to the diabetes-resistant of Rip-B7xAI4αβ mice. PD-1 is a negative regulator of effector T cells (32) and a high level of PD-1 on the surface of CD8 T cells induces cell exhaustion (33, 34). We observed significant, yet comparable, percentages of PD-1 positive AI4αβ cells in both groups of mice (Fig. 6C). We also looked at the expression of Bcl-2, a molecule involved in CD8 T cell survival and death (35). Again, intracellular staining showed a similar level of Bcl-2 protein in AI4αβ cells in both groups of mice (Fig. 6C). These results are consistent with the microarray data and suggest that AI4αβ CD8 T cells in both Rip-B7xAI4αβ and AI4αβ mice have a similar functional status.

Proliferation and cytotoxic function of AI4αβ CD8 T cells in Rip-B7xAI4αβ mice

Given that all AI4αβ mice developed diabetes and died whereas Rip-B7xAI4αβ mice were healthy, we next examined whether AI4αβ CD8 T cells in Rip-B7xAI4αβ mice were fully functional. We purified AI4αβ cells from mice and examined their cytotoxic activity with MimA2 peptide-pulsed C57BL/6.$H2^{g7/g7}$ splenocytes as targets. AI4αβ T cells in Rip-B7xAI4αβ and AI4αβ mice showed similar CTL activity (Fig. 7A), suggesting that AI4αβ T cells in Rip-B7xAI4αβ mice maintain normal cytotoxic function. We further examined *in vivo* AI4αβ T cell proliferation by measuring intracellular Ki-67, a cell proliferation marker. Single-cell suspensions prepared from the pancreas, pancreatic lymph node, and spleen were stained with MimA2/H2-D^b tetramer and an anti-CD8 Ab to detect AI4αβ cells, as well as an anti-Ki-67 Ab to identify proliferating cells. We found that AI4αβ CD8 T cells in AI4αβ mice had greater proliferation than those in RIP-B7xAI4αβ mice (Fig. 7B), but showed a similar percentages of cell death in both groups of mice (Fig. 7C). These data suggest that B7x inhibits antigen specific CD8 T cell proliferation *in vivo* but does not affect the cell death of those pathogenic cells. These results also indicate that the resistance of Rip-B7xAI4αβ mice to diabetes is partially due to the inhibitory effect of B7x on proliferation of pathogenic CD8 T cells.

Discussion

The expression of B7x protein has been reported inconsistently, with some studies showing B7x is induced on some immune cells (2, 3) whereas others reporting immune cells are B7x negative (36). To resolve these discrepancies, we used multiple specific monoclonal and polyclonal antibodies to inspect B7x protein on immune cells. Although extensively examined, we were unable to detect B7x protein in human and mice immune cells under

NIH-PA Author Manuscript

NIH-PA Author Manuscript

NIH-PA Author Manuscript

various stimulations and during infection or cancer. Therefore, we concluded that B7x protein was not expressed in immune cells. By contrast, canonical members of the B7 family such as B7-1 and B7-2 are highly expressed in APCs (37) and activated T cells (38). B7h (ICOS ligand) is also expressed in APCs (39, 40). Whereas PD-L2 (B7-DC) expression is mostly restricted to DCs and macrophages (41), PD-L1 (B7-H1) is widely expressed on hematopoietic cells (41, 42) and several parenchymal tissues (43, 44). B7-H3 can be induced on DCs, monocytes, and lymphocytes (45–47). We now revealed that, unlike any other B7 family members, B7x protein was not expressed on immune cells. This finding has an important implication to understand the *in vivo* function of B7x.

Immune tolerance is maintained through a series of checkpoints that govern in both the thymus and the periphery (48, 49). We and others show that B7x protein is expressed in mice pancreatic β cells and in human pancreas (21) and that B7x can inhibit CD4 T cell-mediated diabetes and experimental autoimmune encephalomyelitis (4). We now further revealed that B7x expressed in pancreatic β cells had an important role in CD8 T cell-mediated pancreas specific damage. B7x−/−AI4αβ mice exhibited even more aggressive disease than AI4αβ mice. As a consequence, B7x−/−AI4αβ mice developed earlier lethality than AI4αβ. These findings unveil a crucial immunosuppressive checkpoint in which tissue-expressed B7x can inhibit self-reactive, tissue-specific CD8 T cells and thus prevent an autoimmune disorder. Given that B7x is not expressed in immune cells, these observations also imply a B7x-dependent suppressive mechanism that operates at the effector T cell phase, not at the stage of T cell priming. As the loss of B7x expression resulted in more severe diabetes, we also examined whether the overexpression of the molecule could prevent disease. We found that the overexpression of B7x in the pancreatic islet β-cells of AI4αβ mice resulted in complete abrogation of diabetes. However, the overexpression of B7x did not prevent insulitis. Rather, islet antigen-specific CD8 T cells were activated in pancreatic lymph node and further migrated into the pancreas in B7x-transgenic mice. Indeed, in two adoptive transfer models of diabetes, the injection of activated diabetogenic CD8 T cells into B7x-transgenic animals generated insulitis but failed to induce diabetes. These results emphasize the inhibitory effect of B7x on pathogenic effector CD8 T cells.

The pathogenesis of most autoimmune diseases involves multiple steps. In T1D, the insulitis phase can persist for long periods of time in humans and mice; many such pre-diabetic individuals never progress to overt diabetes. It is unclear which mechanisms control the conversion from the pre-diabetes insulitis to the diabetic state. As overexpression of B7x in the β cells did not prevent insulitis but abrogated the progression to disease, it is conceivable that the level of B7x protein in the pancreas may be one of the factors that determine whether the insulitis phase proceeds to the diabetic state. It is known that immune cells capable of recognizing self-antigens exist in some normal individuals without causing harmful diseases. Future investigation is clearly warranted to dissect whether coinhibitory B7 molecules, such as B7x or PD-L1, prevent self-reactive immune cells in these individuals from progressing to disease by up-regulating their expression in tissue cells.

Multiple mechanisms have been proposed for the peripheral tolerance of self-reactive CD8 T cells, including anergy (50), clonal deletion (50), and exhaustion (34). In the absence of the B7-1/B7-2/CD28 pathway, antigen encounter can result in T cell anergy or deletion, whereas strong signaling of the PD-L1/PD-1 pathway can convert effector CD8 T cells into exhaustion. Importantly, CD8 T cells acquire overlapping, yet divergent molecular signatures depending on whether they are undergoing anergy, deletion, or exhaustion (35, 51). CD8 T cells undergoing deletion exhibit GzmB and Bcl-2 down-regulation (35), whereas exhausted CD8 T cells overexpress several inhibitory receptors including PD-1 and have major changes in pathways of T cell receptor and cytokine signaling (51). To address the molecular mechanisms of B7x–mediated inhibition of CD8 T cells, we compared the

NIH-PA Author Manuscript

NIH-PA Author Manuscript

NIH-PA Author Manuscript

gene-expression profiles of antigen-specific pancreatic AI4αβ CD8 T cells. Unexpectedly, pancreatic CD8 T cells in diabetic AI4αβ mice and diabetes-free Rip-B7xAI4αβ mice had a similar pattern of global gene expression. CCL3 was the only gene whose expression was statistically higher in the AI4αβ T cells of Rip-B7xAI4αβ mice. In NOD mice, the temporal expression of CCL3 in the pancreas is associated with the development of T1D (52). In human, serum level of CCL3 is increased while CCL2 is decreased in the islet autoantibody-positive group relative to the autoantibody-negative group (53). These studies demonstrate that CCL3 expression increases during the progression to T1D. However, it is unclear whether increased CCL3 is a consequence of inflammation or CCL3 itself promotes disease during T1D development. Most mature hematopoietic cells including T cells and many tissue cells including β-cells produce CCL3 (54), and whether this molecule produced by CD8 T cells has a role in the pathogenesis of diabetes is currently unknown and is open for further investigation with cell type specific CCL3-deficient mouse models. Interestingly, a recent study shows that B7x-Ig protein prevents T-cell proliferation and IL-2 production by inhibiting phosphorylation of ERK, JNK, p38, and AKT, but not LCK or ZAP-70 (55), suggesting that the B7x pathway is able to rapidly interfere with the activation state of some key kinases in the CD28 pathway without markedly changing gene transcription.

Although pancreatic CD8 T cells in Rip-B7xAI4αβ mice were not under immune tolerance as these cells were able to kill target cells very well, AI4αβ T cells in RIP-B7xAI4αβ mice showed less proliferation than those in AI4αβ mice. Moreover, Rip-B7x mice had fewer AI4 CD8 T cells in the pancreas in both spontaneous and adoptive transfer diabetes models. Therefore, what emerges is a model suggesting that B7x in the periphery prevents autoimmune diseases partially by limiting the proliferation of self-reactive, tissue-specific effector CD8 T cells in target tissues. Recent studies show that expression of B7x in islets or an insulinoma cell line prolongs allograft survival (56, 57) and that B7x-Ig fusion protein reduces diabetes incidence in NOD mice (58). Clearly, further studies on this new B7 pathway may lead to novel immunotherapy against autoimmune diseases.

Supplementary Material

Refer to Web version on PubMed Central for supplementary material.

Acknowledgments

We thank Bill Heath (University of Melbourne) for in vitro CTL generation, the Teresa DiLorenzo laboratory (Albert Einstein College of Medicine) for technical help, and the NIH Tetramer Core Facility for generating tetramer.

This work was supported in part by grants from the National Institutes of Health (DP2DK083076 to X.Z., T32DK007513 to K.A.H., T32DK007513 to Y.M.A., P60DK020541 to Diabetes Research Center, and P30CA013330 to Cancer Center) and the Department of Defense (PC094137 to X.Z.).

References

1. Zang X, Loke P, Kim J, Murphy K, Waitz R, Allison JP. B7x: a widely expressed B7 family member that inhibits T cell activation. Proc Natl Acad Sci U S A. 2003; 100:10388–10392. [PubMed: 12920180]
2. Prasad DV, Richards S, Mai XM, Dong C. B7S1, a novel B7 family member that negatively regulates T cell activation. Immunity. 2003; 18:863–873. [PubMed: 12818166]
3. Sica GL, Choi IH, Zhu G, Tamada K, Wang SD, Tamura H, Chapoval AI, Flies DB, Bajorath J, Chen L. B7-H4, a molecule of the B7 family, negatively regulates T cell immunity. Immunity. 2003; 18:849–861. [PubMed: 12818165]
4. Wei J, Loke P, Zang X, Allison JP. Tissue-specific expression of B7x protects from CD4 T cell-mediated autoimmunity. J Exp Med. 2011; 208:1683–1694. [PubMed: 21727190]

NIH-PA Author Manuscript

NIH-PA Author Manuscript

NIH-PA Author Manuscript

5. Rai E, Wakeland EK. Genetic predisposition to autoimmunity--what have we learned? Semin Immunol. 2011; 23:67–83. [PubMed: 21288738]
6. Scandiuzzi L, Ghosh K, Zang X. T cell costimulation and coinhibition: Genetics and disease. Discov Med. 2011; 12:119–128. [PubMed: 21878189]
7. Todd JA. Etiology of type 1 diabetes. Immunity. 2010; 32:457–467. [PubMed: 20412756]
8. Rainbow DB, Moule C, Fraser HI, Clark J, Howlett SK, Burren O, Christensen M, Moody V, Steward CA, Mohammed JP, Fusakio ME, Masteller EL, Finger EB, Houchins JP, Naf D, Koentgen F, Ridgway WM, Todd JA, Bluestone JA, Peterson LB, Mattner J, Wicker LS. Evidence that Cd101 Is an Autoimmune Diabetes Gene in Nonobese Diabetic Mice. J Immunol. 2011; 187:325–336. [PubMed: 21613616]
9. Hinks A, Barton A, Shephard N, Eyre S, Bowes J, Cargill M, Wang E, Ke X, Kennedy GC, John S, Worthington J, Thomson W. Identification of a novel susceptibility locus for juvenile idiopathic arthritis by genome-wide association analysis. Arthritis Rheum. 2009; 60:258–263. [PubMed: 19116933]
10. Bottema RW, Postma DS, Reijmerink NE, Thijs C, Stelma FF, Smit HA, van Schayck CP, Brunekreef B, Koppelman GH, Kerkhof M. Interaction of T-cell and antigen presenting cell co-stimulatory genes in childhood IgE. Eur Respir J. 2010; 35:54–63. [PubMed: 19574333]
11. DiLorenzo TP, Graser RT, Ono T, Christianson GJ, Chapman HD, Roopenian DC, Nathenson SG, Serreze DV. Major histocompatibility complex class I-restricted T cells are required for all but the end stages of diabetes development in nonobese diabetic mice and use a prevalent T cell receptor alpha chain gene rearrangement. Proc Natl Acad Sci U S A. 1998; 95:12538–12543. [PubMed: 9770521]
12. Lieberman SM, Takaki T, Han B, Santamaria P, Serreze DV, DiLorenzo TP. Individual nonobese diabetic mice exhibit unique patterns of CD8+ T cell reactivity to three islet antigens, including the newly identified widely expressed dystrophia myotonica kinase. J Immunol. 2004; 173:6727–6734. [PubMed: 15557165]
13. Choisy-Rossi CM, Holl TM, Pierce MA, Chapman HD, Serreze DV. Enhanced pathogenicity of diabetogenic T cells escaping a non-MHC gene-controlled near death experience. J Immunol. 2004; 173:3791–3800. [PubMed: 15356126]
14. Ratzinger G, Baggers J, de Cos MA, Yuan J, Dao T, Reagan JL, Munz C, Heller G, Young JW. Mature human Langerhans cells derived from CD34+ hematopoietic progenitors stimulate greater cytolytic T lymphocyte activity in the absence of bioactive IL-12p70, by either single peptide presentation or cross-priming, than do dermal-interstitial or monocyte-derived dendritic cells. J Immunol. 2004; 173:2780–2791. [PubMed: 15294997]
15. Loke P, Allison JP. PD-L1 and PD-L2 are differentially regulated by Th1 and Th2 cells. Proc Natl Acad Sci U S A. 2003; 100:5336–5341. [PubMed: 12697896]
16. Loke P, MacDonald AS, Robb A, Maizels RM, Allen JE. Alternatively activated macrophages induced by nematode infection inhibit proliferation via cell-to-cell contact. Eur J Immunol. 2000; 30:2669–2678. [PubMed: 11009101]
17. Weber SE, Tian H, Pirofski LA. CD8+ cells enhance resistance to pulmonary serotype 3 Streptococcus pneumoniae infection in mice. J Immunol. 2011; 186:432–442. [PubMed: 21135172]
18. Takaki T, Lieberman SM, Holl TM, Han B, Santamaria P, Serreze DV, DiLorenzo TP. Requirement for both H-2Db and H-2Kd for the induction of diabetes by the promiscuous CD8+ T cell clonotype AI4. J Immunol. 2004; 173:2530–2541. [PubMed: 15294969]
19. Sheehy ME, McDermott AB, Furlan SN, Klenerman P, Nixon DF. A novel technique for the fluorometric assessment of T lymphocyte antigen specific lysis. J Immunol Methods. 2001; 249:99–110. [PubMed: 11226468]
20. Zang X, Sullivan PS, Soslow RA, Waitz R, Reuter VE, Wilton A, Thaler HT, Arul M, Slovin SF, Wei J, Spriggs DR, Dupont J, Allison JP. Tumor associated endothelial expression of B7-H3 predicts survival in ovarian carcinomas. Mod Pathol. 2010; 23:1104–1112. [PubMed: 20495537]
21. Tringler B, Zhuo S, Pilkington G, Torkko KC, Singh M, Lucia MS, Heinz DE, Papkoff J, Shroyer KR. B7-h4 is highly expressed in ductal and lobular breast cancer. Clin Cancer Res. 2005; 11:1842–1848. [PubMed: 15756008]

NIH-PA Author Manuscript

NIH-PA Author Manuscript

NIH-PA Author Manuscript

22. Graser RT, DiLorenzo TP, Wang F, Christianson GJ, Chapman HD, Roopenian DC, Nathenson SG, Serreze DV. Identification of a CD8 T cell that can independently mediate autoimmune diabetes development in the complete absence of CD4 T cell helper functions. J Immunol. 2000; 164:3913–3918. [PubMed: 10725754]

23. Gagnerault MC, Luan JJ, Lotton C, Lepault F. Pancreatic lymph nodes are required for priming of beta cell reactive T cells in NOD mice. J Exp Med. 2002; 196:369–377. [PubMed: 12163565]

24. Turley S, Poirot L, Hattori M, Benoist C, Mathis D. Physiological beta cell death triggers priming of self-reactive T cells by dendritic cells in a type-1 diabetes model. J Exp Med. 2003; 198:1527–1537. [PubMed: 14623908]

25. Zhang Y, O'Brien B, Trudeau J, Tan R, Santamaria P, Dutz JP. In situ beta cell death promotes priming of diabetogenic CD8 T lymphocytes. J Immunol. 2002; 168:1466–1472. [PubMed: 11801690]

26. Thomas HE, Trapani JA, Kay TW. The role of perforin and granzymes in diabetes. Cell Death Differ. 2010; 17:577–585. [PubMed: 19927156]

27. von Herrath MG, Oldstone MB. Interferon-gamma is essential for destruction of beta cells and development of insulin-dependent diabetes mellitus. J Exp Med. 1997; 185:531–539. [PubMed: 9053453]

28. Kay TW, Campbell IL, Oxbrow L, Harrison LC. Overexpression of class I major histocompatibility complex accompanies insulitis in the non-obese diabetic mouse and is prevented by anti-interferon-gamma antibody. Diabetologia. 1991; 34:779–785. [PubMed: 1722764]

29. Suk K, Kim S, Kim YH, Kim KA, Chang I, Yagita H, Shong M, Lee MS. IFN-gamma/TNF-alpha synergism as the final effector in autoimmune diabetes: a key role for STAT1/IFN regulatory factor-1 pathway in pancreatic beta cell death. J Immunol. 2001; 166:4481–4489. [PubMed: 11254704]

30. Kelchtermans H, Billiau A, Matthys P. How interferon-gamma keeps autoimmune diseases in check. Trends Immunol. 2008; 29:479–486. [PubMed: 18775671]

31. Flaishon L, Topilski I, Shoseyov D, Hershkoviz R, Fireman E, Levo Y, Marmor S, Shachar I. Cutting edge: anti-inflammatory properties of low levels of IFN-gamma. J Immunol. 2002; 168:3707–3711. [PubMed: 11937520]

32. Francisco LM, Sage PT, Sharpe AH. The PD-1 pathway in tolerance and autoimmunity. Immunol Rev. 2010; 236:219–242. [PubMed: 20636820]

33. Barber DL, Wherry EJ, Masopust D, Zhu B, Allison JP, Sharpe AH, Freeman GJ, Ahmed R. Restoring function in exhausted CD8 T cells during chronic viral infection. Nature. 2006; 439:682–687. [PubMed: 16382236]

34. Hofmeyer KA, Jeon H, Zang X. The PD-1/PD-L1 (B7-H1) pathway in chronic infection-induced cytotoxic T lymphocyte exhaustion. J Biomed Biotechnol. 2011; 2011:451694. [PubMed: 21960736]

35. Parish IA, Rao S, Smyth GK, Juelich T, Denyer GS, Davey GM, Strasser A, Heath WR. The molecular signature of CD8+ T cells undergoing deletional tolerance. Blood. 2009; 113:4575–4585. [PubMed: 19204323]

36. Kamimura Y, Kobori H, Piao J, Hashiguchi M, Matsumoto K, Hirose S, Azuma M. Possible involvement of soluble B7-H4 in T cell-mediated inflammatory immune responses. Biochem Biophys Res Commun. 2009; 389:349–353. [PubMed: 19723502]

37. Hathcock KS, Laszlo G, Pucillo C, Linsley P, Hodes RJ. Comparative analysis of B7-1 and B7-2 costimulatory ligands: expression and function. J Exp Med. 1994; 180:631–640. [PubMed: 7519245]

38. Prabhu Das MR, Zamvil SS, Borriello F, Weiner HL, Sharpe AH, Kuchroo VK. Reciprocal expression of co-stimulatory molecules, B7-1 and B7-2, on murine T cells following activation. Eur J Immunol. 1995; 25:207–211. [PubMed: 7531145]

39. Liang L, Porter EM, Sha WC. Constitutive expression of the B7h ligand for inducible costimulator on naive B cells is extinguished after activation by distinct B cell receptor and interleukin 4 receptor-mediated pathways and can be rescued by CD40 signaling. J Exp Med. 2002; 196:97–108. [PubMed: 12093874]

NIH-PA Author Manuscript

NIH-PA Author Manuscript

NIH-PA Author Manuscript

40. Aicher A, Hayden-Ledbetter M, Brady WA, Pezzutto A, Richter G, Magaletti D, Buckwalter S, Ledbetter JA, Clark EA. Characterization of human inducible costimulator ligand expression and function. J Immunol. 2000; 164:4689–4696. [PubMed: 10779774]
41. Yamazaki T, Akiba H, Iwai H, Matsuda H, Aoki M, Tanno Y, Shin T, Tsuchiya H, Pardoll DM, Okumura K, Azuma M, Yagita H. Expression of programmed death 1 ligands by murine T cells and APC. J Immunol. 2002; 169:5538–5545. [PubMed: 12421930]
42. Ishida M, Iwai Y, Tanaka Y, Okazaki T, Freeman GJ, Minato N, Honjo T. Differential expression of PD-L1 and PD-L2, ligands for an inhibitory receptor PD-1, in the cells of lymphohematopoietic tissues. Immunol Lett. 2002; 84:57–62. [PubMed: 12161284]
43. Liang SC, Latchman YE, Buhlmann JE, Tomczak MF, Horwitz BH, Freeman GJ, Sharpe AH. Regulation of PD-1, PD-L1, and PD-L2 expression during normal and autoimmune responses. Eur J Immunol. 2003; 33:2706–2716. [PubMed: 14515254]
44. Mazanet MM, Hughes CC. B7-H1 is expressed by human endothelial cells and suppresses T cell cytokine synthesis. J Immunol. 2002; 169:3581–3588. [PubMed: 12244148]
45. Chapoval AI, Ni J, Lau JS, Wilcox RA, Flies DB, Liu D, Dong H, Sica GL, Zhu G, Tamada K, Chen L. B7-H3: a costimulatory molecule for T cell activation and IFN-gamma production. Nat Immunol. 2001; 2:269–274. [PubMed: 11224528]
46. Suh WK, Gajewska BU, Okada H, Gronski MA, Bertram EM, Dawicki W, Duncan GS, Bukczynski J, Plyte S, Elia A, Wakeham A, Itie A, Chung S, Da Costa J, Arya S, Horan T, Campbell P, Gaida K, Ohashi PS, Watts TH, Yoshinaga SK, Bray MR, Jordana M, Mak TW. The B7 family member B7-H3 preferentially down-regulates T helper type 1-mediated immune responses. Nat Immunol. 2003; 4:899–906. [PubMed: 12925852]
47. Steinberger P, Majdic O, Derdak SV, Pfistershammer K, Kirchberger S, Klauser C, Zlabinger G, Pickl WF, Stockl J, Knapp W. Molecular characterization of human 4Ig-B7-H3, a member of the B7 family with four Ig-like domains. J Immunol. 2004; 172:2352–2359. [PubMed: 14764704]
48. Goodnow CC. Multistep pathogenesis of autoimmune disease. Cell. 2007; 130:25–35. [PubMed: 17632054]
49. Walker LS, Abbas AK. The enemy within: keeping self-reactive T cells at bay in the periphery. Nat Rev Immunol. 2002; 2:11–19. [PubMed: 11908514]
50. Redmond WL, Sherman LA. Peripheral tolerance of CD8 T lymphocytes. Immunity. 2005; 22:275–284. [PubMed: 15780985]
51. Wherry EJ, Ha SJ, Kaech SM, Haining WN, Sarkar S, Kalia V, Subramaniam S, Blattman JN, Barber DL, Ahmed R. Molecular signature of CD8+ T cell exhaustion during chronic viral infection. Immunity. 2007; 27:670–684. [PubMed: 17950003]
52. Cameron MJ, Arreaza GA, Grattan M, Meagher C, Sharif S, Burdick MD, Strieter RM, Cook DN, Delovitch TL. Differential expression of CC chemokines and the CCR5 receptor in the pancreas is associated with progression to type I diabetes. J Immunol. 2000; 165:1102–1110. [PubMed: 10878389]
53. Hanifi-Moghaddam P, Kappler S, Seissler J, Muller-Scholze S, Martin S, Roep BO, Strassburger K, Kolb H, Schloot NC. Altered chemokine levels in individuals at risk of Type 1 diabetes mellitus. Diabet Med. 2006; 23:156–163. [PubMed: 16433713]
54. Maurer M, von Stebut E. Macrophage inflammatory protein-1. Int J Biochem Cell Biol. 2004; 36:1882–1886. [PubMed: 15203102]
55. Wang X, Hao J, Metzger DL, Ao Z, Chen L, Ou D, Verchere CB, Mui A, Warnock GL. B7-H4 Treatment of T Cells Inhibits ERK, JNK, p38, and AKT Activation. PLoS One. 2012; 7:e28232. [PubMed: 22238573]
56. Yuan CL, Xu JF, Tong J, Yang H, He FR, Gong Q, Xiong P, Duan L, Fang M, Tan Z, Xu Y, Chen YF, Zheng F, Gong FL. B7-H4 transfection prolongs beta-cell graft survival. Transpl Immunol. 2009; 21:143–149. [PubMed: 19361556]
57. Wang X, Hao J, Metzger DL, Mui A, Ao Z, Verchere CB, Chen L, Ou D, Warnock GL. Local expression of B7-H4 by recombinant adenovirus transduction in mouse islets prolongs allograft survival. Transplantation. 2009; 87:482–490. [PubMed: 19307783]

58. Wang X, Hao J, Metzger DL, Mui A, Ao Z, Akhoundsadegh N, Langermann S, Liu L, Chen L, Ou D, Verchere CB, Warnock GL. Early Treatment of NOD Mice With B7-H4 Reduces the Incidence of Autoimmune Diabetes. Diabetes. 2011; 60:3246–3255. [PubMed: 21984581]

Abbreviations used in this article

APCs	antigen-presenting cells
Idd	insulin-dependent diabetes loci
T1D	Type 1 diabetes.

NIH-PA Author Manuscript
NIH-PA Author Manuscript
NIH-PA Author Manuscript

NIH-PA Author Manuscript
NIH-PA Author Manuscript
NIH-PA Author Manuscript

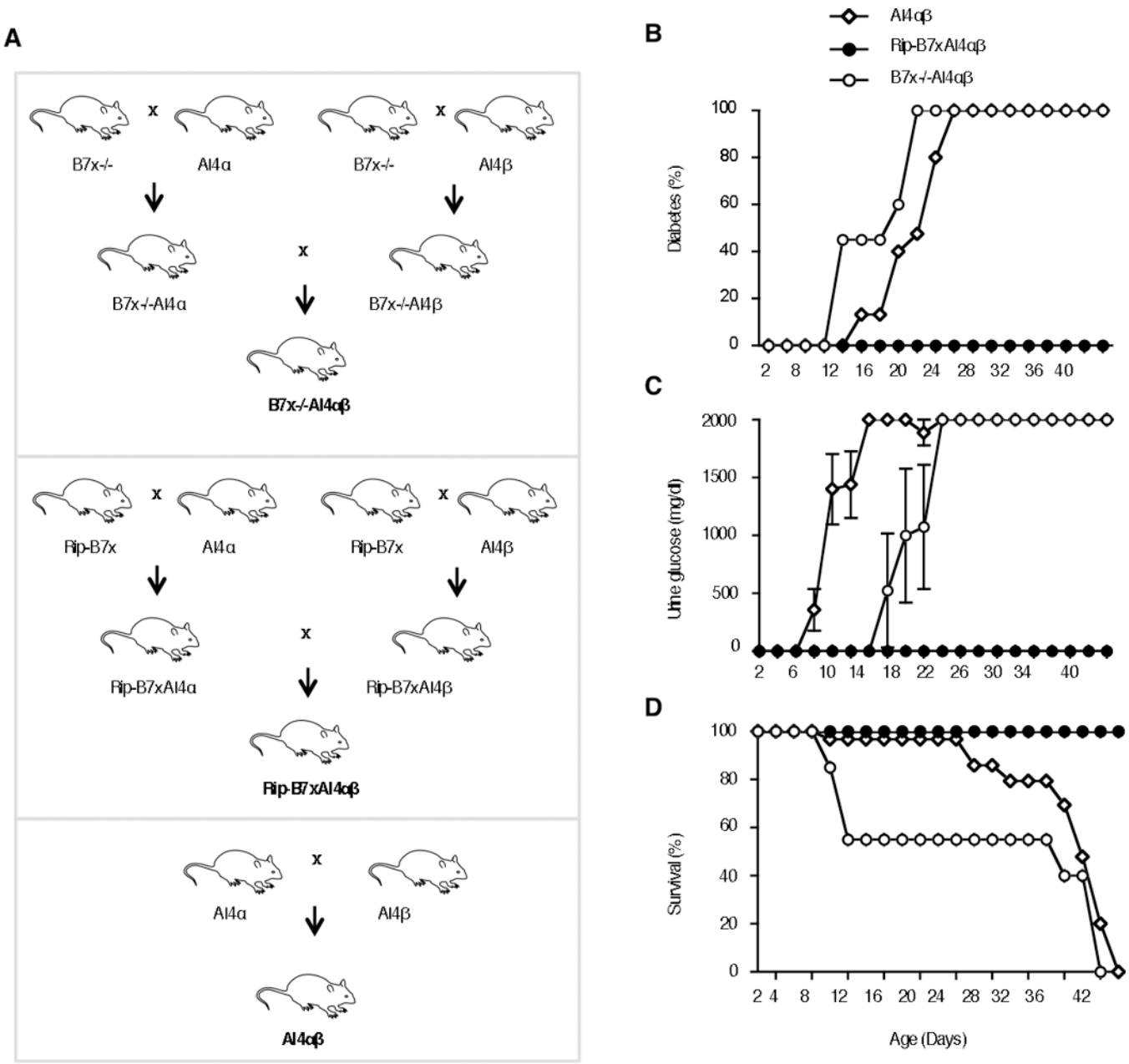

FIGURE 1.

B7x deficiency leads to exacerbated diabetes whereas B7x overexpression in pancreatic β cells abrogates disease induced by CD8 T cells recognizing an endogenous self-antigen in the pancreas. (**A**) Scheme for generation of B7x−/−AI4αβ, Rip-B7xAI4αβ and AI4αβ mice on C57BL/6.H2$^{g7/g7}$ background. (**B–D**) B7x−/−AI4αβ, Rip-B7xAI4αβ, and control AI4αβ mice were examined for diabetes incidence (B), glucose measurements (C), and survival (D); n = 8–10 mice per group. Data are representative of three independent experiments and are presented as means ± S.E.M.

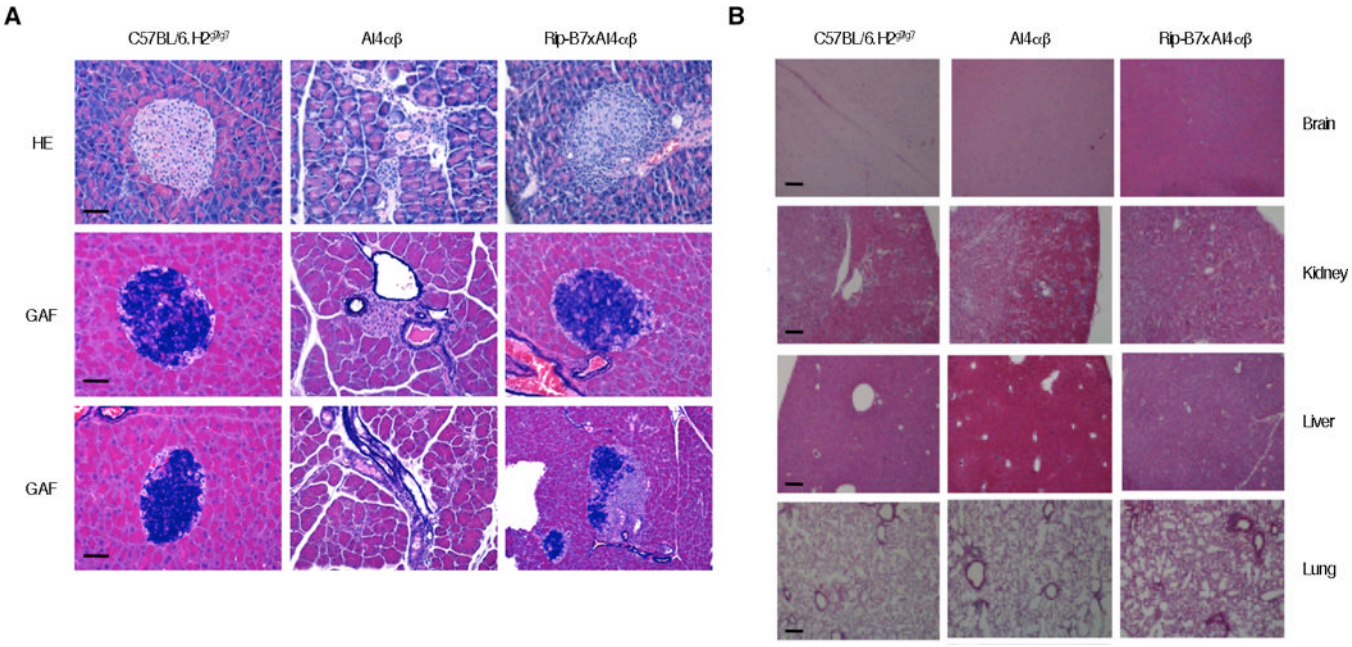

FIGURE 2.

Pathogenic CD8 T cells infiltrate into the pancreas in B7x-transgenic mice. (**A**) HE and GAF stained pancreatic sections from C57BL/6.H2$^{g7/g7}$, AI4αβ, and RIP-B7xAI4αβ mice. Scale bar 50 μm, magnification 20×. (**B**) HE stained sections of brain, kidney, liver, and lung fromC57BL/6.H2$^{g7/g7}$, AI4αβ, and RIP-B7xAI4αβ mice. Scale bar 200 μm, magnification 5×. n = 3–5 mice per group, data represent one of three independent experiments.

NIH-PA Author Manuscript NIH-PA Author Manuscript NIH-PA Author Manuscript

NIH-PA Author Manuscript

NIH-PA Author Manuscript

NIH-PA Author Manuscript

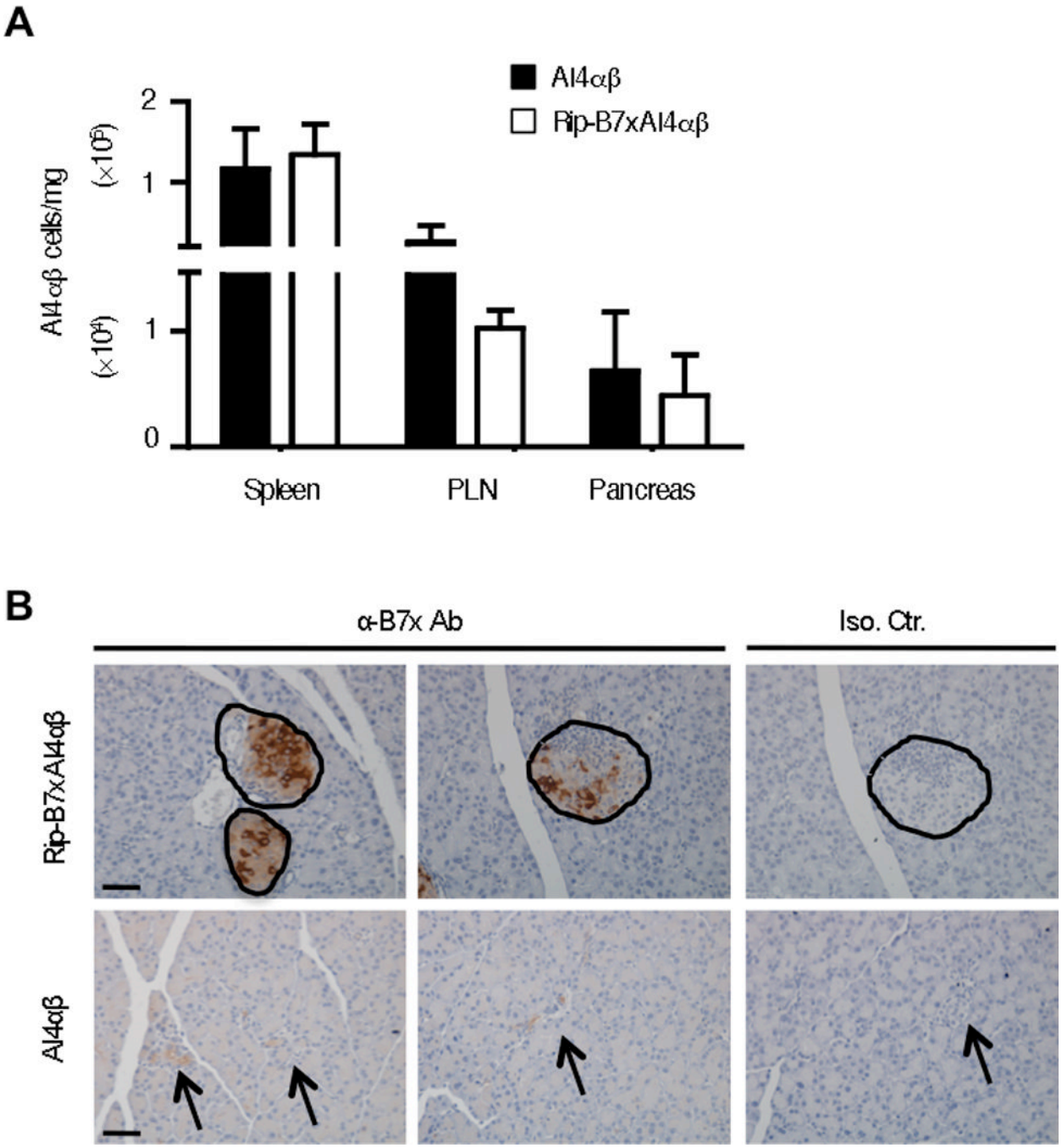

FIGURE 3.

Leukocytic infiltrates and B7 expression in islets of B7x-transgenic mice. (**A**) Absolute number of AI4αβ CD8 T cells normalized to weight of spleen, pancreatic lymph node (PLN), and pancreas from AI4αβ and RIP-B7xAI4αβ mice. AI4αβ CD8 T cells were determined by MimA2/H2-D^b tetramer and anti-CD8 staining. n = 3–5 mice per group; data are presented as means ± SEM and they represent one of three independent experiments. (**B**) Representative pictures of immunohistochemistry staining with anti-B7x Ab and isotype control in pancreatic tissue sections of AI4αβ and RIP-B7xAI4αβ mice. Some islets of Rip-B7xAI4αβ mice had leukocytic infiltrates where B7x-positive cells were confined to areas

devoid of infiltrates. Islets in AI4αβ mice were barely detectable with no obvious staining for B7x. Hematoxylin staining of nuclei in images is blue, Ab-specific staining of B7x is brown. Scale bar 50μm, magrification 20×. Circles and arrows indicate islets.

NIH-PA Author Manuscript
NIH-PA Author Manuscript
NIH-PA Author Manuscript

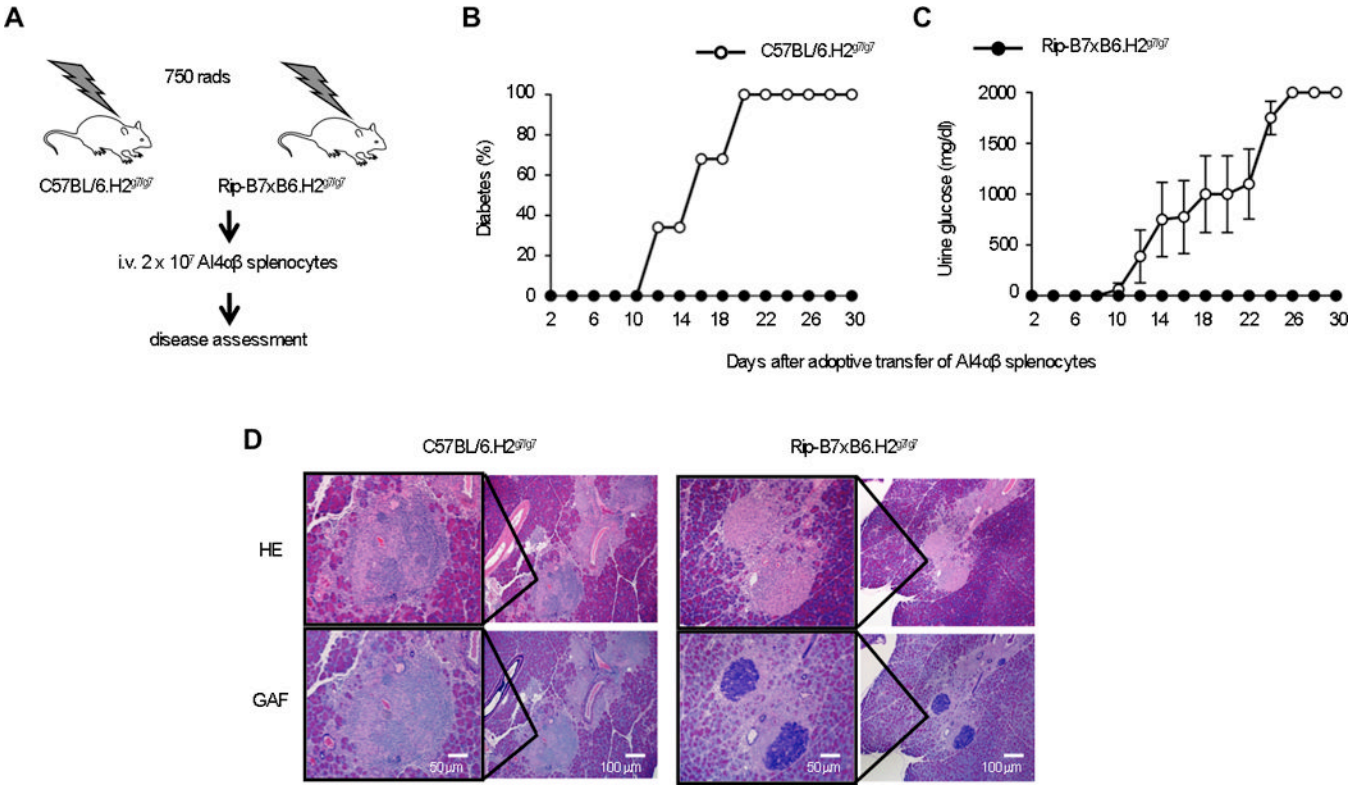

FIGURE 4.

Irradiated Rip-B7x mice do not develop diabetes after adoptive transfer of effector AI4αβ CD8 T cells. (**A**) Scheme of adoptive transferred AI4αβ splenocytes-induced diabetes in irradiated recipients. (**B–C**) Irradiated Rip-B7xB6.H2$^{g7/g7}$ mice and control C57BL/6.H2$^{g7/g7}$ mice were intravenously injected with splenocytes from AI4αβ mice and monitored for diabetes development including diabetes incidence (B) and urine glucose level (C). (**D**) Representative pictures of HE and GAF stained pancreatic tissue sections 30 days after adopted transfer of AI4αβ cells in Rip-B7xB6.H2$^{g7/g7}$ mice and C57BL/6.H2$^{g7/g7}$ mice. Scale bars, 50 μm, magnification 20× (left panels); 100 μm, magnification 10x (right panels). Data are presented as means ± SEM and they represent one of four independent experiments; n=10 per group.

NIH-PA Author Manuscript NIH-PA Author Manuscript NIH-PA Author Manuscript

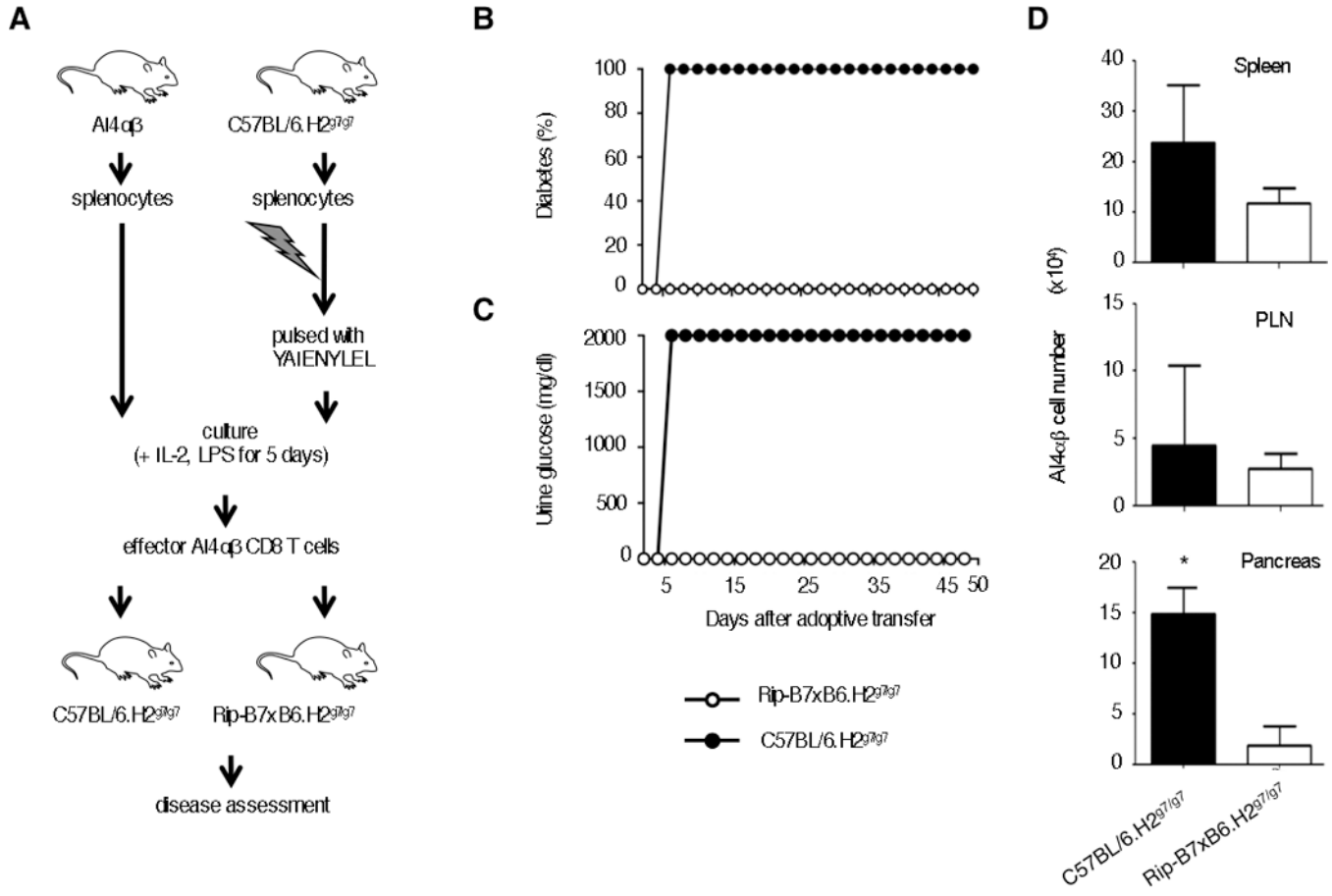

FIGURE 5.

B7x inhibits effector CD8 T cell-induced diabetes. (**A**) Scheme for adoptive transfer of effector CD8 T cell-induced diabetes in naïve mice. (**B–C**) Naive Rip-B7xB6.H2$^{g7/g7}$ mice and control C57BL/6.H2$^{g7/g7}$ mice were intravenously injected with effector AI4αβ CD8 T cells and monitored for diabetes development including diabetes incidence (B) and urine glucose level (C). (**D**) Absolute number of AI4αβ cells in spleen, pancreatic lymph node (PLN), and pancreas from C57BL/6.H2$^{g7/g7}$ mice and Rip-B7xB6.H2$^{g7/g7}$ mice 30 days after adoptive transfer of effector CD8 T cells. Data are shown as mean ± SEM (n=10 per group) and they represent one of three independent experiments. * p <0.05 by Student t test.

NIH-PA Author Manuscript NIH-PA Author Manuscript NIH-PA Author Manuscript

NIH-PA Author Manuscript

NIH-PA Author Manuscript

NIH-PA Author Manuscript

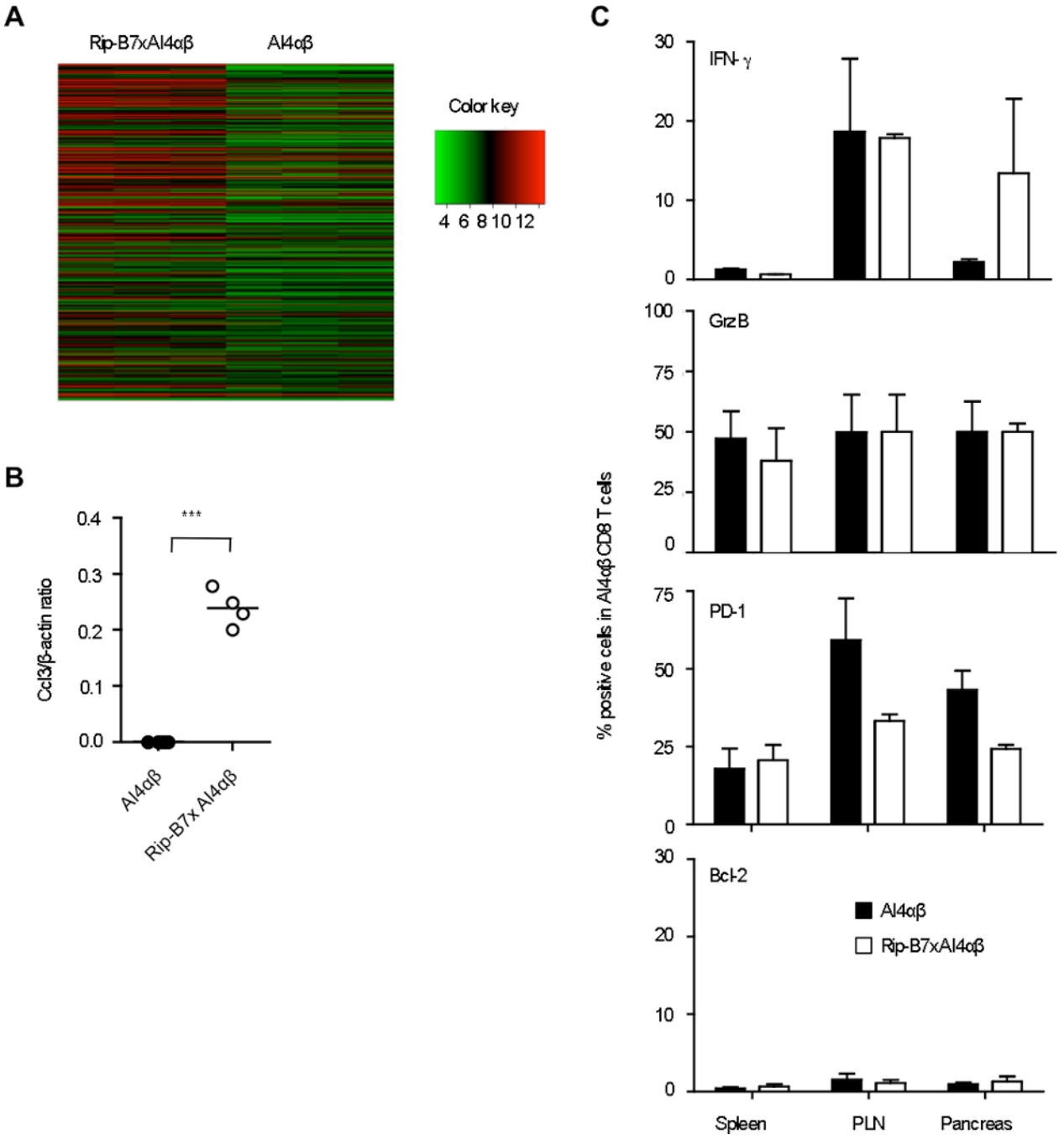

FIGURE 6.

Comparison of global gene expression profiles and effector functional proteins in pancreatic CD8 T cells. (**A**) Hierarchical clustering analysis for top 500 genes with the lowest adjusted p value in pancreatic AI4αβ CD8 T cells from Rip-B7xAI4αβ and AI4αβ mice, three replicates per group are shown. (**B**) RT-PCR determination of mRNAs for CCL3 and the housekeeping gene β-actin in pancreatic AI4αβ cells isolated from AI4αβ and Rip-B7xAI4αβ mice at 4–5 weeks of age. (**C**) Flow cytometry analysis of cell surface PD-1 and intracellular IFN-γ, GrzB, and Bcl-2 expressed by AI4αβ cells in spleen, pancreatic lymph node (PLN), and pancreas from RIP-B7xAI4αβ and AI4αβ mice. AI4αβ CD8 T cells were

determined by MimA2/H2-D^b tetramer and anti-CD8 staining. Data are shown as mean ± SEM (n=3–4 per group) of two independent experiments. ***p <0.001.

NIH-PA Author Manuscript
NIH-PA Author Manuscript
NIH-PA Author Manuscript

NIH-PA Author Manuscript
NIH-PA Author Manuscript
NIH-PA Author Manuscript

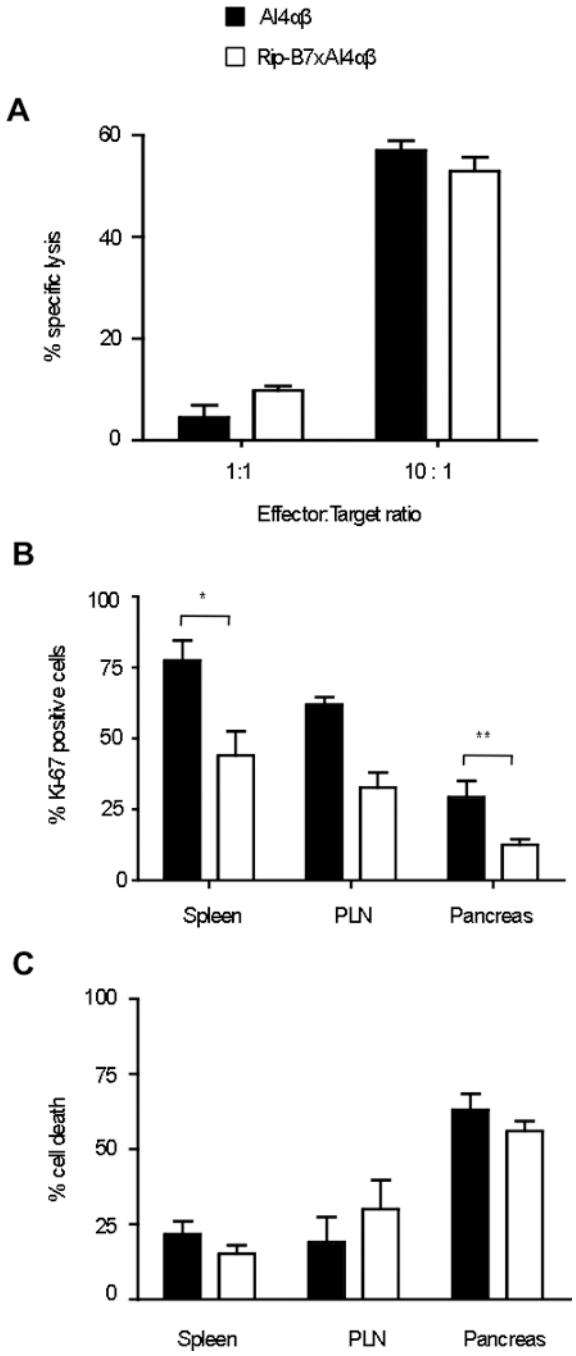

FIGURE 7.

Cytotoxic function, proliferation, and cell death of AI4αβ CD8 T cells. (**A**) AI4αβ CD8 T cell cytotoxic response toward target cells of MimA2 peptide-pulsed C57BL/6.H2$^{g7/g7}$ splenocytes. (**B**) Percentage of AI4αβ T cells that expressed Ki-67 in spleen, PLN, and pancreas from AI4αβ and RIP-B7xAI4αβ mice. AI4αβ CD8 T cells were determined by MimA2/H2-D^{b} tetramer and anti-CD8 staining. (**C**) Percentage of cell death in AI4αβ CD8 T cells. Data are shown as means ± SEM and they are representative of two to three independent experiments; n = 3–5 mice per group. *p <0.05, **p <0.01 by Student t test.

NIH-PA Author Manuscript

NIH-PA Author Manuscript

NIH-PA Author Manuscript

Table I

B7x protein is not detected in APCs and T cells before and after stimuli

Immune cells	Stimulation and disease models
Human	
Dendritic cells	CD40L, LPS, PMA+ ionomycin, cytokine cocktail
Langerhans cells	CD40L, cytokine cocktail
Monocytes	LPS+IFN-γ
B cells	LPS, PMA+ ionomycin
T cells	PHA, PMA+ ionomycin
Mouse	
Dendritic cells	4T1 cancer, *S pneumoniae* infection, *B malayi* infection,
Macrophages	4T1 cancer, *S pneumoniae* infection, *B malayi* infection,
B cells	LPS, anti-IgM F(ab')2, PMA+ ionomycin, 4T1 cancer, *S pneumoniae* infection
T cells	ConA, anti-CD3/CD28, PMA+ ionomycin, 4T1 cancer, *S pneumoniae* infection Th1, Th2, Treg

B7x protein was examined by flow cytometry with specific monoclonal or polyclonal Abs.